Molecular Therapy
Nucleic Acids
Original Article

AMERICAN SOCIETY of GENE & CELL THERAPY

Long-Term Morpholino Oligomers in Hexose Elicits Long-Lasting Therapeutic Improvements in *mdx* Mice

Gang Han,[1] Caorui Lin,[1] Hanhan Ning,[1] Xianjun Gao,[1] and HaiFang Yin[1]

[1]School of Medical Laboratory and Department of Cell Biology, Tianjin Medical University, Qixiangtai Road, Heping District, Tianjin 300070, China

Approval of antisense oligonucleotide eteplirsen highlights the promise of exon-skipping therapeutics for Duchenne muscular dystrophy patients. However, the limited efficacy of eteplirsen underscores the importance to improve systemic delivery and efficacy. Recently, we demonstrated that a glucose and fructose (GF) delivery formulation effectively potentiates phosphorodiamidate morpholino oligomer (PMO). Considering the clinical potential of GF, it is important to determine the long-term compatibility and efficacy with PMO in *mdx* mice prior to clinical translation. Here, we report that yearlong administration of a clinically applicable PMO dose (50 mg/kg/week for 3 weeks followed by 50 mg/kg/month for 11 months) with GF elicited sustainably high levels of dystrophin expression in *mdx* mice, with up to 45% of the normal level of dystrophin restored in most peripheral muscles without any detectable toxicity. Importantly, PMO-GF resulted in phenotypical rescue and mitochondrial biogenesis with functional improvement. Carbohydrate metabolites measurements revealed improved metabolic and energetic conditions after PMO-GF treatment in *mdx* mice without metabolic anomaly. Collectively, our study shows PMO-GF's ability to elicit long-lasting therapeutic effects with tolerable toxicity and represents a new treatment modality for Duchenne muscular dystrophy, and provides guidelines for antisense oligonucleotides with GF in clinical use.

INTRODUCTION

Antisense oligonucleotide (AO)-mediated exon-skipping therapeutics is one of the most promising approaches for Duchenne muscular dystrophy (DMD), with one AO drug (eteplirsen, registered as Exondys51) with phosphorodiamidate morpholino oligomer (PMO) backbone approved by the US Food and Drug Administration (FDA) in 2016.[1,2] However, the efficacy of eteplirsen, due to insufficient systemic delivery, needs to be improved for affordable clinical use. Although a plethora of delivery systems with appreciable delivery efficiency have been developed, including polymers[3–6] and cell-penetrating peptides (CPPs),[7–10] their safety profiles remain to be established. Therefore, a compatible delivery system for AO drugs or eteplirsen with high translational potential is urgently required for nucleic acid therapeutics. Recently, we identified a delivery formulation, the mixture of glucose and fructose (GF), which showed significant enhancement on the delivery of various AOs, particularly PMO, to muscle in energy-deficient mice such as dystrophin-deficient *mdx* mice.[11,12]

We wished to evaluate four long-term outcomes of the PMO-GF strategy because these are known to be inefficient in some current PMO formulations. First, it was well recognized that systemic delivery of naked PMO is inefficient in *mdx* mice: high doses of PMO were employed in *mdx* mice to achieve therapeutic levels of dystrophin restoration,[1,13–15] and a relatively high dose of eteplirsen resulted in only trace amounts of dystrophin in DMD patients.[1,13–15] Thus, we wanted to evaluate the delivery efficiency of PMO-GF. Second, because AO-mediated exon skipping works on RNA rather than the genome, the therapeutic effect lasts for only a short period of time with a single dose of AO.[16] However, the chronic nature of DMD[17] necessitates us to evaluate whether PMO-GF can maintain functional levels of dystrophin with tolerable toxicity over time. Third, because AOs are presumed to enter muscle cells at least partially through leaky membranes[18] and membrane integrity recovers after treatment, we wanted to evaluate whether the membrane integrity of treated muscles affects delivery of PMO-GF. Fourth, highly heterogeneous dystrophin expression was observed between muscles or intra-muscle at low dosage of AOs, which produced only a limited amount of dystrophin and might not be able to halt the cycles of degeneration.[19,20] Thus, we sought to investigate the distribution and homogeneity of dystrophin expression and the functional improvement elicited by low doses of PMO in GF.

Prior to the identification of the causal gene, *dystrophin* or *Dmd*, DMD was regarded as a metabolic disease manifested by a systemic metabolic impairment, characterized by abnormal and mis-localized mitochondria with changes in cristae and density.[21,22] Because mitochondria are the cell's ATP production machinery, mitochondrial dysfunction triggers a cascade of physiological events, including deficits in cytosolic enzymes of glycolysis and reduced ATP content in

Received 7 April 2018; accepted 14 June 2018;
https://doi.org/10.1016/j.omtn.2018.06.005.

Correspondence: HaiFang Yin, School of Medical Laboratory and Department of Cell Biology, Tianjin Medical University, Qixiangtai Road, Heping District, Tianjin 300070, China.
E-mail: haifangyin@tmu.edu.cn

DMD patients and animal models.[22–24] However, it remains unknown whether dystrophin restoration is sufficient to affect mitochondrial and energetic conditions in *mdx* mice and DMD patients. With discovery of the new role of GF in enhancing PMO delivery to energy-deficient muscles and its clinical implications, it becomes important to investigate whether long-term repeated use of PMO-GF will have an impact on mitochondria and carbohydrate metabolism.

To investigate the long-term clinical applicability of PMO-GF, we administered PMO-GF at clinical applicable dosages with monthly administrations in *mdx* mice for 1 year. Strikingly, functional levels of dystrophin were induced and maintained in most peripheral muscles of *mdx* mice without any detectable toxicity. Dystrophin restoration further stimulated mitochondrial biogenesis and functions. Importantly, yearlong treatment with PMO-GF significantly improved the energetic conditions of *mdx* mice without alteration on carbohydrate metabolic homeostasis. Thus, PMO-GF represents a treatment modality for DMD patients worth exploring in the clinic.

RESULTS

PMO-GF Elicits Long-Lasting Therapeutic Levels of Dystrophin in *mdx* Mice

To determine the clinical applicability and safety of chronic lifelong use of PMO-GF, we intravenously administered PMO-GF at 50 mg/kg/week for 3 weeks followed by 50 mg/kg/month for 11 months in *mdx* mice (Figure 1A). This resulted in a substantial number of dystrophin-positive myofibers in multiple peripheral muscle groups except for the heart (Figure 1B). Strikingly, up to 45% of the normal level of dystrophin was restored in tibialis anterior (TA), quadriceps, gastrocnemius, and abdominal muscles as demonstrated by western blot (Figures 1C and 1D), suggesting that chronic administration of PMO-GF at low dosage enables long-lasting dystrophin restoration and maintenance of therapeutic levels of dystrophin. Examination of the amount of PMOs in muscles from PMO-GF-treated *mdx* mice revealed comparable levels of PMOs in peripheral muscles between yearlong and 6-month treatment (Figure 1E), implying that appreciable amounts of PMO persisted in muscle to induce therapeutic levels of dystrophin restoration.

PMO-GF Maintains Functional Rescue without Detectable Toxicity in *mdx* Mice

PMO-GF-treated *mdx* mice were monitored closely, and no abnormal behavior was observed throughout the year. No abnormal bodyweight increases were observed in PMO-GF-treated *mdx* mice compared with age-matched untreated *mdx* controls (Figure S1A), indicating that a low monthly dose of GF does not cause any weight gain. Correlating with high levels of dystrophin restoration in peripheral muscles from PMO-GF-treated *mdx* mice, pathophysiological improvement was demonstrated by re-localization of dystrophin-associated protein complex (DAPC),[25] which fails to localize accurately to the sarcolemma in the absence of dystrophin (Figure 2A); a significant decline in the level of serum creatine kinase (CK) (Figure 2B), usually elevated in *mdx* mice;[26] a reduction in the percentage of centrally nucleated fibers in myofibers (Figure 2C), an index of ongoing degeneration and regeneration cycles;[27] and reduced fibrosis in peripheral muscles demonstrated by collagen deposition (Figure 2D), compared with age-matched untreated *mdx* controls. Functional rescue was evident from force recovery in the grip strength test, with steady improvement following yearlong PMO-GF treatment compared with age-matched untreated *mdx* controls (Figure 2E). These data demonstrate that yearlong PMO-GF treatment can substantially trigger phenotypic rescue and halt disease progression.

To examine whether PMO-GF evokes any detectable toxicity, we analyzed serum biochemical indices including aspartate aminotransferase (AST), alanine aminotransferase (ALT), alkaline phosphatase (ALP), serum creatinine (Cr), urea, blood urea nitrogen (BUN), and serum glucose. Levels of ALT and AST dramatically declined in *mdx* mice treated with PMO-GF compared with untreated *mdx* controls (Figure 2F), which are elevated in *mdx* mice naturally because of leakage from diseased muscle tissues.[28] No change was found on levels of ALP (Figure 2F), Cr, BUN, and urea (Figure 2G). Consistently, histological examination on liver, kidney, and muscle revealed no abnormal morphological changes as demonstrated by H&E staining (Figures S1B and S1C). No inflammatory cell activation was detected in muscle from *mdx* mice treated with PMO-GF as demonstrated by staining of macrophages (Figure S1D), indicating that yearlong treatment of PMO-GF does not provoke any hepatic and renal toxicity and inflammation. Also, no change was detected in the level of serum glucose in *mdx* mice treated with PMO-GF compared with age-matched *mdx* controls (Figure 2G). These results demonstrate that PMO-GF represents a new therapeutic modality with the capacity to maintain functional levels of dystrophin expression with manageable injections at low doses and tolerable toxicity.

Improved Membrane Integrity Attenuates the Uptake of PMO-GF in Muscle

We next wished to investigate whether PMO-GF maintains its potency after the membrane integrity was improved as PMO enters the cell partially via diffusion through a leaky membrane.[18,26] To determine the integrity of the sarcolemmal membrane, we stained circulating immunoglobulin G (IgG), an indicator for membrane permeability,[29] in quadriceps from *mdx* mice treated with PMO-GF and different ages of *mdx* controls including age-matched (aged) and adult *mdx* mice. As expected, less staining and a significant reduction in fluorescence intensity were observed in quadriceps from *mdx* mice treated with PMO-GF compared with age-matched and adult *mdx* controls (Figures 3A and 3B), indicating that yearlong treatment of PMO-GF improves the sarcolemmal membrane integrity of *mdx* mice. A significant increase in fluorescence intensity in IgG staining in aged *mdx* mice compared with adult *mdx* controls (Figures 3A and 3B) demonstrates age-related IgG accumulation. To understand whether PMO-GF retains its potency in improved sarcolemmal membrane, we intravenously administered lissamine-labeled PMO in GF at the dose of 25 mg/kg for a single injection in *mdx* mice treated with PMO-GF for 1 year (treated) and age-matched (aged) and adult *mdx* controls under identical conditions. Body-wide

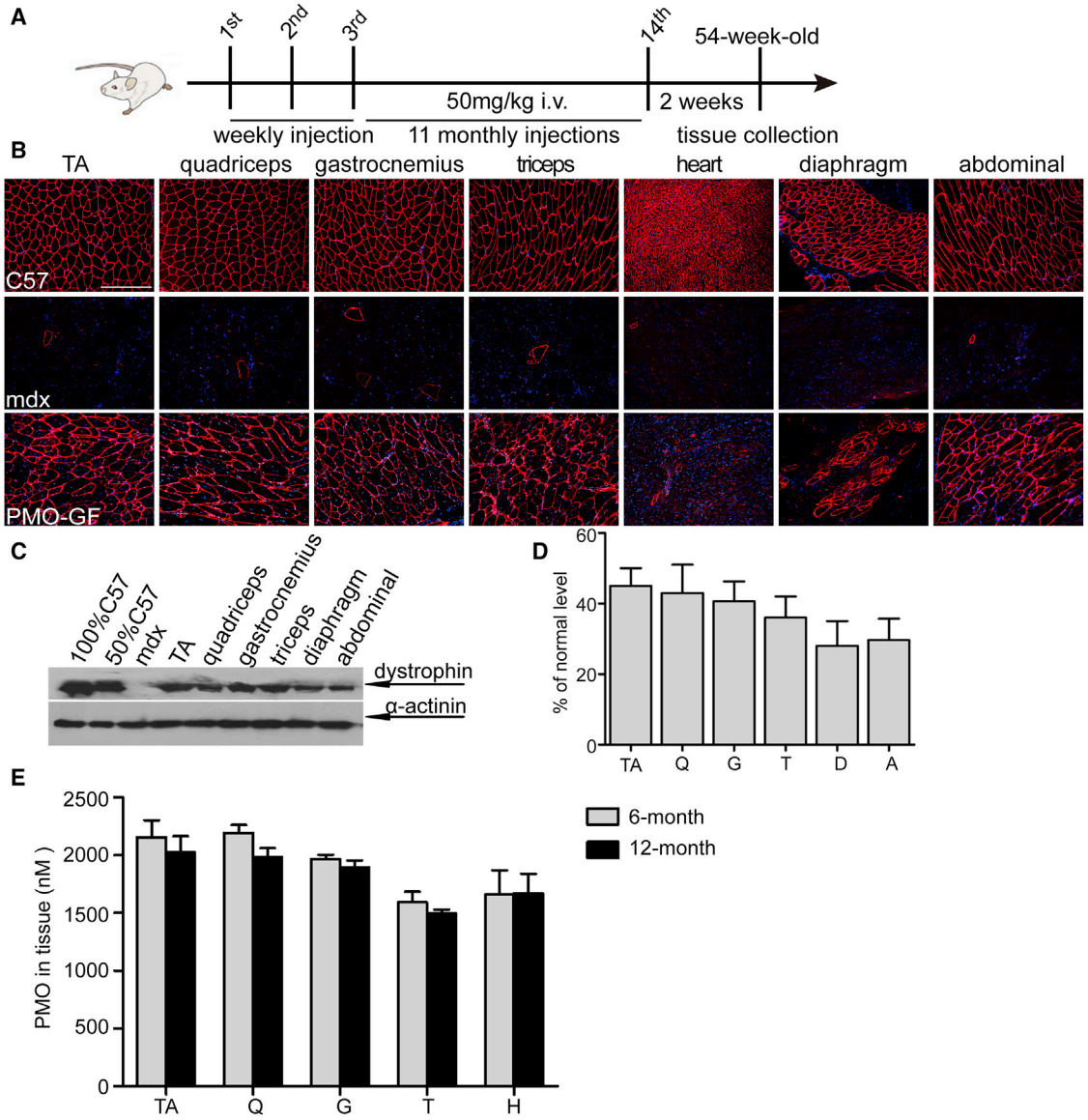

Figure 1. Dystrophin Restoration in *mdx* Mice with Yearlong Systemic Administration of PMO-GF

Dystrophin restoration in *mdx* mice treated with PMO-GF at the dosage of 50 mg/kg/week for 3 weeks followed by 50 mg/kg/month for 11 months intravenously. (A) Diagram to illustrate the dosing regimen and time for tissue collection. (B) Immunohistochemistry for dystrophin expression in body-wide muscles from *mdx* mice treated with PMO-GF (scale bar, 200 μm). (C) Representative western blot image to show dystrophin restoration in *mdx* mice treated with PMO-GF. 12.5, 25, and 50 μg of total protein from *C57BL6* and 50 μg from untreated and treated *mdx* muscle samples were loaded, respectively. α-Actinin was used as the loading control. (D) Quantitative analysis of western blot results with ImageJ. Four biological replicates were examined and quantified based on densitometry as described in the Materials and Methods. The data present as mean + SEM unless otherwise specified (n = 4). (E) Quantification of PMO in muscle tissues with ELISA. No significant difference was detected between 6-month and yearlong treatment of PMO-GF (n = 4). A, abdominal muscle; D, diaphragm; Q, quadriceps; G, gastrocnemius; i.v., intravenous injection; T, triceps; TA, tibialis anterior.

muscles were harvested 48 hr after injection and imaged with IVIS, and the results demonstrated substantially reduced fluorescence signals in tissues from *mdx* mice treated with PMO-GF for 1 year compared with aged-matched and adult *mdx* controls (Figure 3C). Quantitative analysis of fluorescence intensity indicated that significant increases were achieved in abdominal and TA muscles from age-matched *mdx* controls compared with adult *mdx* controls and *mdx* mice treated with PMO-GF for 1 year (Figure 3D), supporting the notion that a leaky membrane contributes to the uptake of naked AOs. Although the uptake of lissamine-labeled PMO was decreased in muscle from treated *mdx* mice compared with untreated *mdx* controls, it was still significantly above background (Figure 3D), suggesting that PMO-GF is capable of entering muscle with improved membrane integrity, although to a lesser extent, possibly through a

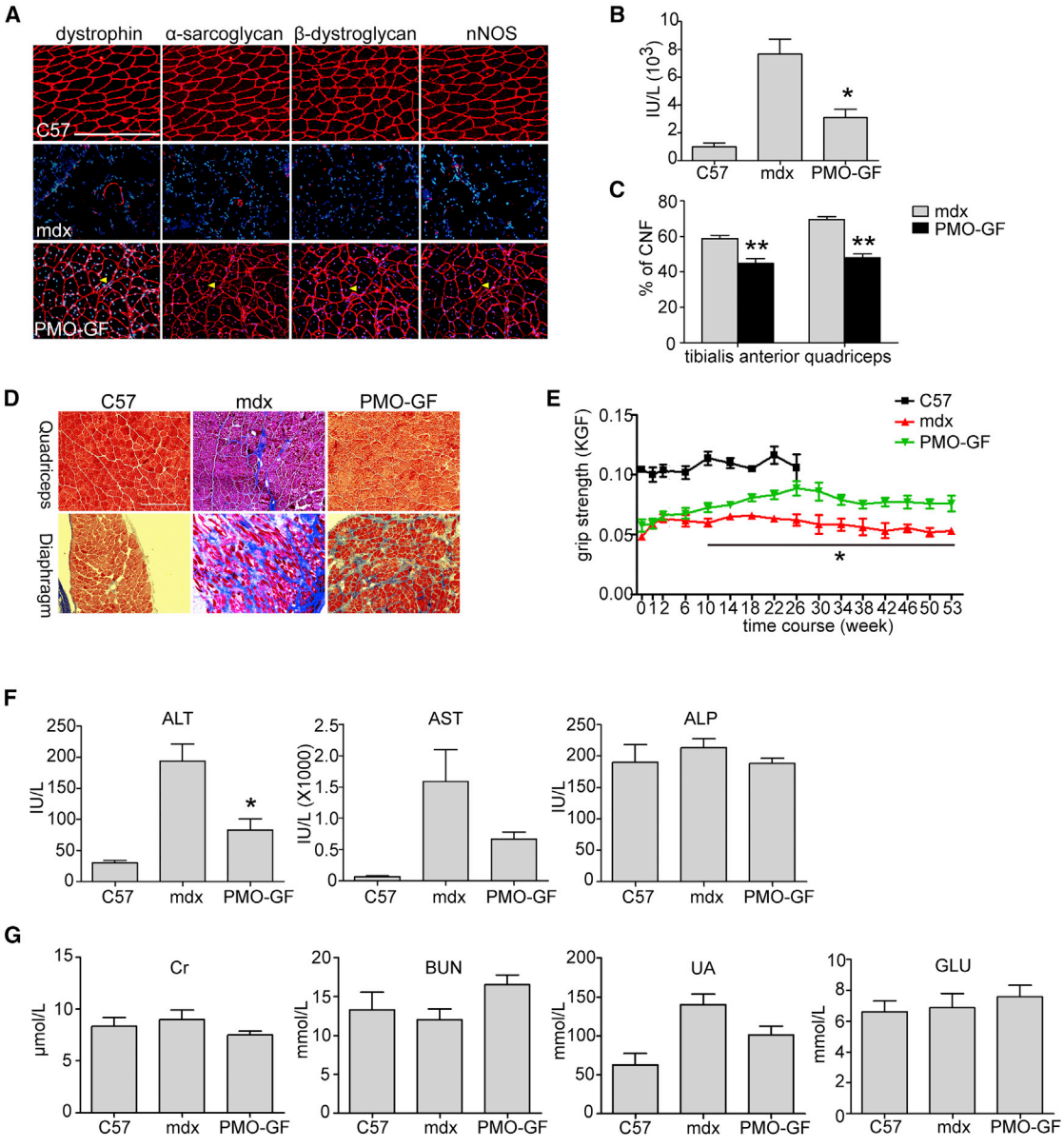

Figure 2. Functional Improvement in *mdx* Mice Treated with PMO-GF for 1 Year

Functional improvement in *mdx* mice treated with PMO-GF at the dosage of 50 mg/kg/week for 3 weeks followed by 50 mg/kg/month for 11 months intravenously. (A) Re-localization of dystrophin-associated protein complex (DAPC) components in treated *mdx* mice to assess dystrophin function and recovery of normal myoarchitecture. (B) Measurement of serum creatine kinase (CK) levels. Data show a significant fall in *mdx* mice treated with PMO-GF compared with untreated age-matched *mdx* controls (two-tailed t test, n = 5, *p < 0.05). (C) Evaluation of CNFs in tibialis anterior and quadriceps from *mdx* mice treated with PMO-GF. A significant decrease was detected between PMO-GF-treated mdx mice and age-matched *mdx* controls (two-tailed t test, n = 5, **p < 0.01). (D) Collagen deposition analysis in diaphragm and quadriceps from *mdx* mice treated with PMO-GF (scale bar, 200 μm). (E) Muscle function was assessed to determine the physical improvement. A significant improvement was detected between PMO-GF-treated *mdx* mice and untreated age-matched *mdx* controls at different time points (two-tailed t test, n = 5, *p < 0.05). (F) Measurement of serum levels of liver enzymes in *mdx* mice treated with PMO-GF compared with untreated *mdx* controls. Data show improved pathological parameters in *mdx* mice treated with PMO-GF compared with untreated age-matched *mdx* controls (two-tailed t test, n = 5, *p < 0.05). (G) Analysis of biochemical indicators for kidney function and glucose in *mdx* mice treated with PMO-GF. Data show no difference in the level of serum creatinine (Cr), BUN, urea, and glucose in *mdx* mice treated with PMO-GF compared with untreated *mdx* and normal controls (n = 5).

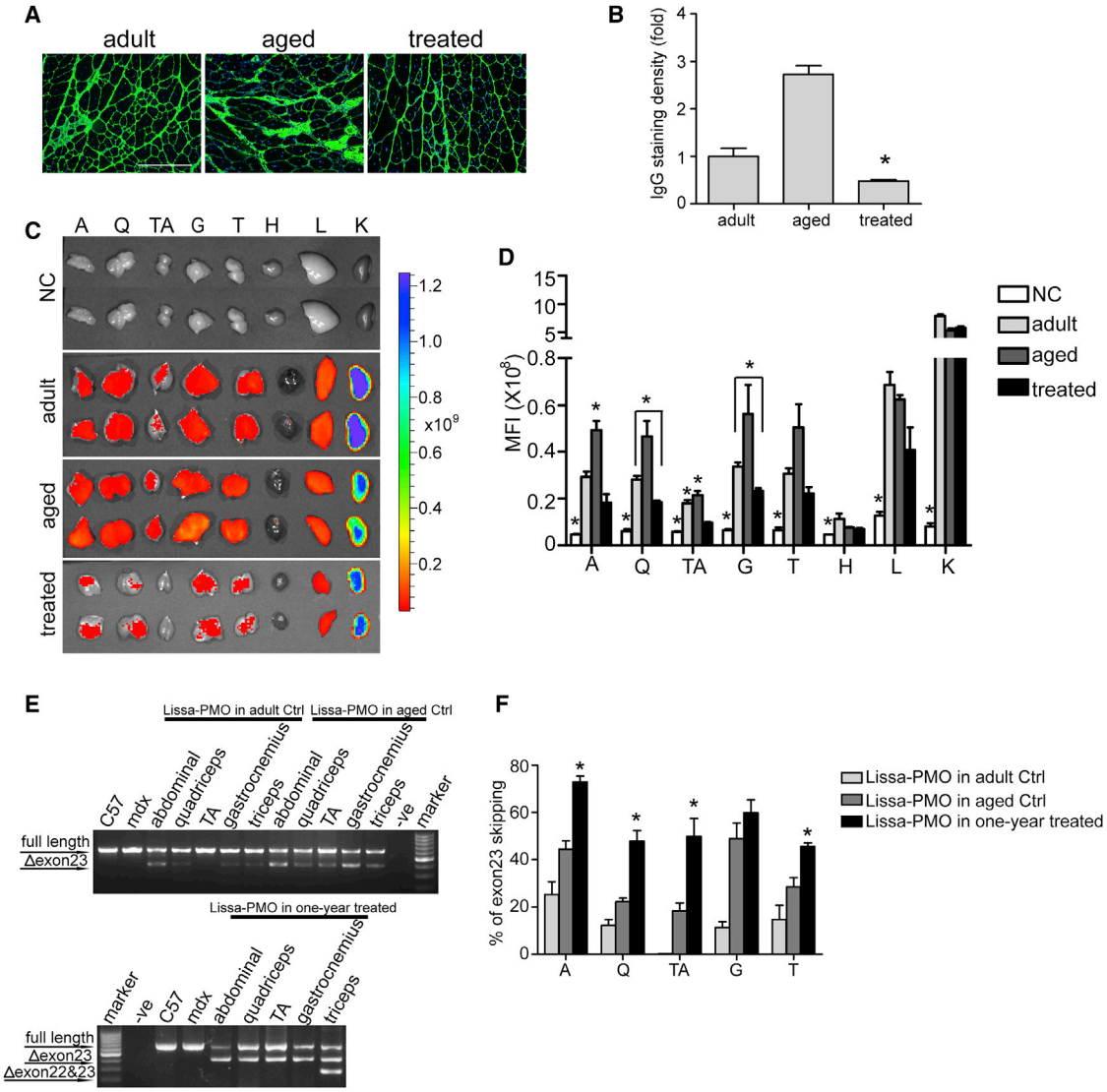

Figure 3. Analysis of Membrane Integrity and Tissue Distribution in *mdx* Mice Treated with PMO-GF

(A) IgG staining to assess the membrane integrity in quadriceps from *mdx* mice treated with PMO-GF (treated) and untreated age-matched (aged) and adult (adult) *mdx* controls (scale bar, 200 μm). (B) Quantitative analysis of IgG fluorescence intensity in quadriceps from *mdx* mice treated with PMO-GF and untreated age-matched and adult *mdx* controls (n = 3, *p < 0.05). (C) Tissue distribution of lissamine-labeled PMO in body-wide tissues from *mdx* mice with IVIS spectrum series. Body-wide tissues were harvested 48 hr after a single intravenous injection of lissamine-labeled PMO-GF at the dose of 25 mg/kg/day for 1 day. Lissamine (Lissa)-PMO+GF in adult control (Ctrl), Lissa-PMO+GF in aged Ctrl, and Lissa-PMO+GF in 1-year treated represents adult, aged *mdx* controls, or 1-year-treated *mdx* mice injected with a single dose of lissamine-labeled PMO in GF. (D) Quantitative evaluation of fluorescence intensity in body-wide tissues from *mdx* mice treated with lissamine-labeled PMO in GF. Significant differences were detected in untreated *mdx* controls (NC) compared with other groups (n = 3; *p < 0.05), and significant differences were detected in A and TA from age-matched *mdx* controls (aged) compared with adult and PMO-GF treated *mdx* mice (n = 3; *p < 0.05). Significant differences were detected in Q, G, and TA from adult *mdx* mice compared with PMO-GF-treated *mdx* mice (n = 3; *p < 0.05). (E) RT-PCR to determine the level of exon skipping in muscles treated with lissamine-labeled PMO in GF at 25mg/kg for a single injection. Δexon 23 or Δexon 22&23 for exon 23 or exons 22 and 23 skipped bands, respectively. (F) Quantitative analysis of exon 23 skipping efficiency. Significant increases in levels of exon skipping were found in A, Q, TA, and triceps from *mdx* mice treated with PMO-GF for 1 year compared with age-matched and adult *mdx* controls (n = 3; *p < 0.05). Significance was determined with two-tailed t test. A, abdominal muscle; G, gastrocnemius; H, heart; K, kidney; L, liver; NC, untreated controls; Q, quadriceps; T, triceps; TA, tibialis anterior; treated, *mdx* mice treated with PMO-GF for 1 year.

mechanism independent of membrane leakage. Examination of exon-skipping efficiency revealed significant increases in levels of exon 23 skipping in abdominal muscles, quadriceps, TA, and triceps from PMO-GF-treated *mdx* mice compared with aged-matched and adult *mdx* controls with a single injection of PMO-GF (Figures 3E and 3F), further strengthening the conclusion that the PMO reservoir in *mdx*

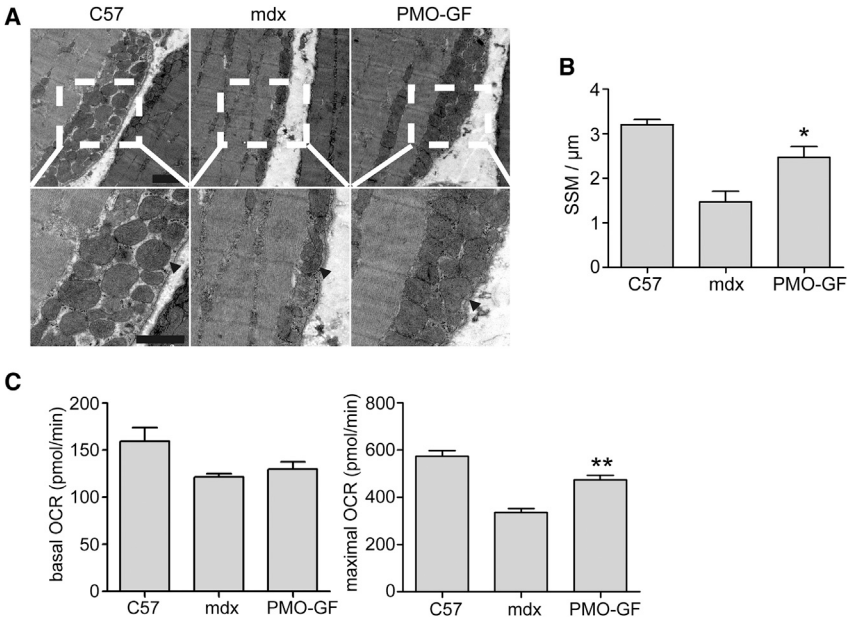

Figure 4. Dystrophin Restoration Increases Subsarcolemmal Mitochondria Pool Density in *mdx* Mice Treated with PMO-GF for 1 Year

(A) Transmission electron microscopy micrographs of the SSM pool in tibialis anterior skeletal muscles from wild-type *C57BL6*, age-matched untreated *mdx* controls, and PMO-GF-treated *mdx* mice (scale bars, 1 μm). Arrowheads point to SSMs. (B) Quantitative analysis of SSM densities. Number of mitochondria per micron length of sarcolemma was determined from transmission electron micrographs. In both wild-type *C57BL6* and PMO-GF-treated *mdx* mice skeletal muscle, SSMs were heavily concentrated along the subsarcolemmal space and averaged around three SSMs per micron of sarcolemma. SSM density in PMO-GF-treated *mdx* mice was significantly increased compared with aged-matched untreated *mdx* controls (two-tailed t test, n = 5, *p < 0.05). (C) Measurement of basal and maximal oxygen consumption rate (OCR) in skeletal muscles from *mdx* mice treated with PMO-GF for 1 year. Data show a significant reduction at the maximal OCR in *mdx* mice treated with PMO-GF compared with untreated *mdx* controls (two-tailed t test, n = 5, **p < 0.01).

mice is likely responsible for the increased exon-skipping efficiency. These findings demonstrate that the potency of PMO-GF attenuates with the membrane integrity improved.

PMO-GF Improves Mitochondrial Biogenesis and Functions in *mdx* Mice

Mitochondrial structure and localization are compromised in dystrophin-deficient patients and *mdx* mice.[30–32] Mitochondria consists of two distinct pools, with one located beneath the sarcolemma (subsarcolemmal) and another at the I band and intermyofibrillar space of the contractile apparatus (intermyofibrillar).[33] In *mdx* skeletal muscle, a decrease in the density of subsarcolemmal mitochondria (SSMs) around necrotic and regenerating fibers was observed.[34,35] Also, swollen mitochondria are evident in *mdx* skeletal muscle.[30,36] Because dystrophin is important in maintaining SSM pool density,[21] we examined the density and localization of SSMs in TA muscles from *mdx* mice treated with PMO-GF with transmission electron microscopy. An orderly assembly and a significantly increased pool density of SSMs were observed in TA muscles from PMO-GF-treated *mdx* mice compared with age-matched *mdx* controls (Figures 4A and 4B). Consistently, ultrastructural analysis of intermyofibrillar mitochondria exhibited long trains of mitochondrial pools in the intermyofibrillar space in TA muscles from PMO-GF-treated *mdx* mice (Figure S2). These data demonstrate that dystrophin restoration stimulates mitochondrial biogenesis. Cellular oxygen consumption is commonly recognized as a fundamental measurement of mitochondrial function,[30] in which mitochondrial oxygen consumption is coupled with the electron transport chain, and thus contributes to ATP production under normal physiological conditions. Whereas mitochondrial uncoupling agents such as carbonyl cyanide-4 (trifluoromethoxy) phenylhydrazone (FCCP) can uncouple oxygen consumption from ATP production in the mitochondria and increase the energy demand, and thus stimulate the respiratory chain to operate at maximum capacity; therefore, maximal oxygen consumption rate (OCR) is used as an indicator for mitochondrial function.[37] To investigate whether mitochondrial functions can be improved in the presence of dystrophin, we measured basal OCR, an indicator for coupled mitochondrial respiration and uncoupled consumption of oxygen,[38] and maximal OCR, an index for coupled and uncoupled respiration provoked by addition of FCCP,[37] in quadriceps from *mdx* mice treated with PMO-GF. A significantly higher level of maximal OCR was achieved in PMO-GF-treated *mdx* mice compared with age-matched untreated *mdx* controls, although to a much less extent with basal OCR (Figure 4C), indicating the improved ability of muscle cells to respond to increased energy demand. Altogether, these findings indicate that PMO-GF treatment can improve mitochondrial biogenesis and functions.

PMO-GF Replenishes Energy Stores without Metabolic Anomaly

Because severely reduced ATP content was observed in skeletal muscle from both DMD patients and *mdx* mice,[22,23,30,32] we next wished to investigate whether the energy conditions can be improved in *mdx* mice with chronic treatment of PMO-GF. Corroborating with improved mitochondria functions, a significant increase in ATP levels was achieved in TA and quadriceps from PMO-GF-treated *mdx* mice compared with age-matched untreated *mdx* controls (Figure 5A). In line with the increased level of ATP, evident rises in AMP and ADP levels were observed in muscle from *mdx* mice treated with PMO-GF with liquid chromatography tandem-mass spectrometry (LC-MS/MS) (Figure 5B). NAD is a cofactor at multiple sites of the tricarboxylic acid (TCA) cycle and in glycolysis, and contributes to the generation of the mitochondrial membrane potential, which is

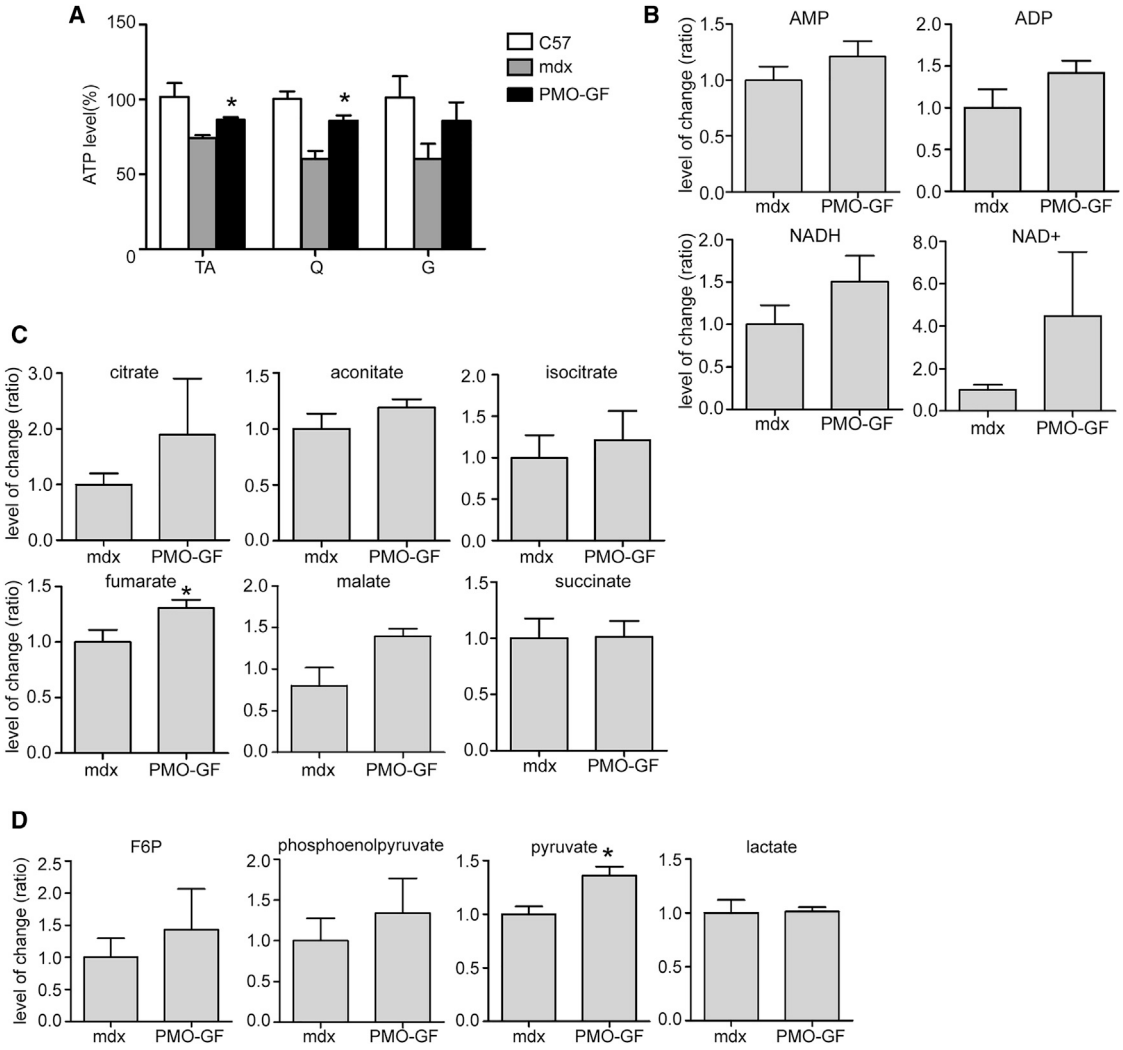

Figure 5. Investigation of Energetic and Carbohydrate Metabolic Conditions in PMO-GF-Treated *mdx* Mice

(A) Measurement of ATP levels in *mdx* mice treated with PMO-GF for 1 year. Significant differences were achieved in energy stores in TA and Q from *mdx* mice treated with PMO-GF compared with untreated age-matched *mdx* controls (n = 5; *p < 0.05). (B) Analysis of levels of AMP, ADP, NADH, and NAD^+ in skeletal muscles from *mdx* mice treated with PMO-GF. (C) Assessment of key components in the TCA cycle with LC-MS/MS. A significant rise was detected in fumarate in *mdx* mice treated with PMO-GF compared with untreated age-matched *mdx* controls (n = 5; *p < 0.05). (D) Measurement of intermediates in glycolytic pathways in skeletal muscles from *mdx* mice treated with PMO-GF. A significant increase was detected in pyruvate in *mdx* mice treated with PMO-GF compared with untreated age-matched *mdx* controls (n = 5; *p < 0.05). Significance was determined with two-tailed t test.

the driving force for ATP production.[39] Because the total NAD pool was decreased in the dystrophic muscle,[40] we analyzed NAD and NADH levels in muscle. Consistent with the ATP data, an evident increase in levels of both NAD and NADH was found in muscle from PMO-GF-treated *mdx* mice compared with age-matched untreated *mdx* controls (Figure 5B). Due to mitochondrial dysfunction in DMD patients and *mdx* mouse muscles, it appeared that some enzymes of the TCA cycle function abnormally, which results in decreased production of certain components at the TCA level.[41,42] Strikingly, substantial increases were detected in different components of the TCA cycle with fumarate showing a significant rise compared with the equivalent in age-matched untreated *mdx* controls, whereas citrate and malate rose to lesser extents (Figure 5C), suggesting that improved mitochondrial function contributes to metabolic homeostasis at the TCA level. Reduced pyruvate kinase activities were observed in DMD patients and *mdx* muscle samples, which result in lower levels of pyruvate.[43,44] To determine whether the long-term chronic treatment of PMO-GF will have an impact on carbohydrate metabolism, we analyzed different key substrates in the glycolytic pathway. Importantly, a significant rise in the level of pyruvate was observed in muscle from PMO-GF-treated *mdx* mice compared with age-matched untreated *mdx* controls

(Figure 5D), whereas there was no significant change found in other intermediates including fructose 6-phosphate (F6P), phosphoenolpyruvate, and lactate in the glycolytic pathway (Figure 5D). Collectively, these data demonstrate that PMO-GF treatment can replenish energy stores without perturbing carbohydrate metabolic homeostasis.

DISCUSSION

Exon-skipping therapeutics represents a promising strategy for DMD with one AO drug approved.[1,2] However, low systemic efficacy presents a huge obstacle for clinical use of the approved drug, which can be potentially resolved with clinically applicable and compatible delivery formulations. Recently, we identified a delivery formulation, GF, which can significantly potentiate the activities of DMD AOs.[11] Even though the potency of PMO-GF was established in our previous study, therapy for DMD requires a life-long treatment, and the ability of therapeutics to maintain functional levels of dystrophin with tolerable toxicity is critical for its clinical translation. Therefore, in the present study, we treated *mdx* mice with PMO-GF for 1 year with a low dosage (50 mg/kg) and monthly administration. Because 6-month treatment with GF alone (3 weekly + 5 monthly repeated intravenous injections) did not result in any improvement in functional outcomes (grip strength and energy levels) in *mdx* mice compared with untreated age-matched *mdx* controls in our previous study,[11] yearlong and less frequent administration of GF alone (3 weekly + 11 monthly intravenous injections) will unlikely have any impact on metabolic parameters; therefore, GF alone was not included in the present study. Strikingly, approximately 50% of the normal level of dystrophin was restored in peripheral muscles from *mdx* mice treated with about 17 mg of PMO in total, a comparable improvement that was only observed with bi-weekly injections of PMO at 1.5 g/kg,[15] without any detectable toxicity. The yearlong treatment of PMO-GF also elicited phenotypic rescue and functional improvement in *mdx* mice as demonstrated by force recovery and re-localization of DAPC and improved membrane integrity. Mitochondrial biogenesis and functions were also stimulated, resulting in increased levels of ATP and components in the TCA cycle without perturbing carbohydrate metabolic homeostasis. In summary, our findings provide evidence for the first time that PMO-GF is capable of maintaining therapeutic levels of dystrophin restoration with low dosage without any detectable toxicity, and thus can be fast-tracked to the clinic for DMD treatment.

It is interesting to note that comparable amounts of PMO were detected in body-wide peripheral muscles from *mdx* mice treated with PMO-GF for 6 months or 1 year, suggesting that the half-life of PMO in muscle is much longer than we assumed, and the long half-life likely contributes to the maintenance of therapeutic levels of dystrophin restoration. Also, it is possible that GF somehow stabilize PMO in muscle, or the improved sarcolemmal membrane integrity contributes to the retention of PMO in muscle. Another possibility is that the restoration of dystrophin expression is partially responsible for the long half-life of PMO in muscle.[15] Intriguingly, we also detected appreciable amounts of PMO in the heart from *mdx* mice treated with PMO-GF for 6 months or 1 year, although there was no dystrophin detected in the heart, implying that a higher threshold concentration or correct localization of PMO might be required to induce detectable dystrophin restoration in the heart, possibly by combining GF with PMOs containing targeting moieties that can enhance delivery to cardiomyocyte nuclei. However, we did observe an evident decline in CK-MB (Figure S3A), a form of enzyme found primarily in heart cells,[45] and decreased staining of IgG (Figure S3B) in PMO-GF-treated *mdx* mice, suggesting that PMO-GF might somehow alleviate the pathologies in the heart. Further studies to explore the effect of GF on the heart are warranted.

It is a concern for exon-skipping therapeutics in DMD if the uptake of PMO declines over time with improved muscle integrity and energetics following dystrophin restoration. Although the uptake of PMO-GF declined with improved membrane integrity, the amount of PMO delivered by GF is sufficient to elicit sustainable and therapeutic levels of dystrophin restoration as demonstrated by high levels of dystrophin expression in body-wide peripheral muscle from *mdx* mice treated with PMO-GF for 1 year, although to a lesser extent than *mdx* mice treated with 6-month repeated injections of PMO-GF.[11] It suggests that likely a minimal amount of PMO is required to maintain the reservoir in muscle once the PMO concentration was built up and the membrane integrity was improved. Thus, PMO-GF shows the ability to maintain the pool and can be used for the life-long treatment of DMD patients.

Strikingly, an evident rise in substrates for ATP production, including ADP, AMP, and NAD, and substantial increases in levels of certain components of the TCA cycle, which are usually decreased in dystrophic muscle due to the reduced activities of corresponding enzymes,[21,42] are likely due to increased metabolic activities in mitochondria. However, we cannot exclude the possibility that the availability of carbohydrate substrates is responsible for this effect and further studies are warranted. Importantly, the long-term chronic treatment restored the level of pyruvate, which is usually reduced in dystrophic muscle because of reduced pyruvate kinase activities,[43,44] without altering other intermediates in glycolysis, suggesting that PMO-GF is beneficial for long-term chronic use in DMD patients without metabolic anomaly.

Altogether, our results show that PMO-GF can be immensely useful for treating DMD patients and manifests the feature essential for the life-long treatment including maintaining therapeutic levels of dystrophin expression at low dosage without any toxicity. The application of PMO-GF can stimulate mitochondrial biogenesis and functions, and re-build the metabolic link without perturbing metabolic homeostasis in muscle. Thus, our study presents a new treatment modality for DMD and other related muscular dystrophies and opens a new avenue for nucleic acid therapeutics.

MATERIALS AND METHODS

Animals and Injections

Adult *mdx* (6- to 8-week-old) and age-matched *C57BL6* mice were used in all experiments (purchased from The Jackson Laboratory,

USA) (four mice per group unless otherwise specified, no gender preference and equal number of male and female mice used for each group). The experiments were carried out in the Animal unit, Tianjin Medical University (Tianjin, China), according to procedures authorized by the institutional ethical committee (permit number: SYXK 2009-0001). For the systemic study, PMO in GF (2.5% glucose: 2.5% fructose) (Sigma, USA) was repeatedly injected at 50 mg/kg/week for 3 weeks followed by 50 mg/kg/month for 11 months in *mdx* mice intravenously. Mice were sacrificed by CO_2 inhalation at 2 weeks after the last injection unless otherwise specified, and muscles and other tissues were snap-frozen in liquid nitrogen-cooled isopentane and stored at −80°C or fixed with Bouin's solution (Sigma, USA) and embedded with paraffin for histological studies.

Oligonucleotides

PMO were synthesized by GeneTools (Corvallis, OR, USA). PMO (5′-ggccaaacctcggcttacctgaaat-3′) sequence was targeted to the murine *dystrophin* exon 23/intron 23 boundary site as reported previously.[46]

RNA Extraction and Nested RT-PCR Analysis

Total RNA was extracted with TRIzol (Invitrogen, UK) as per the manufacturer's instructions, and 200 ng of RNA template was used for 20 μL of RT-PCR with OneStep RT-PCR kit (Qiagen, UK). The primer sequences for the initial RT-PCR were exon 20F0: 5′-CA GAATTCTGCCAATTGCTGAG-3′ and exon 26R0: 5′-TTCTT CAGCTTTTGTGTCATCC-3′ for reverse transcription from mRNA and amplification of cDNA from exons 20–26.[47] The cycling conditions were 95°C for 1 min, 55°C for 1 min, and 72°C for 2 min for 25 cycles. The primer sequences for the second rounds were exon 20F1: 5′-CCCAGTCTACCACCCTATCAGAGC-3′ and exon 24R1: 5′-CCTGCCTTTAAGGCTTCCTT-3′. The cycling conditions were 95°C for 1 min, 57°C for 1 min, and 72°C for 1 min for 25 cycles. The products were examined by electrophoresis on a 2% agarose gel.

Immunohistochemistry and Histology

Series of 8 μm sections were examined for dystrophin, DAPC, and macrophages with series of polyclonal and monoclonal antibodies as described elsewhere.[38] Routine H&E staining was used to examine liver and kidney morphology. For the IgG immune staining, goat anti-mouse IgG Alex Fluor 488 secondary antibody (1:200) was used as reported elsewhere.[29] The extent of the area containing IgG-positive myofibers was measured by ImageJ in three different muscle sections per mouse. For each section, we calculated the ratio between positive area and the total area of the section. The average from three different sections per mouse was calculated and plotted on the graph.

Centrally Nucleated Fiber Counts

The number of centrally nucleated muscle fibers in TA and quadriceps muscles from *mdx* mice treated with weekly (for 3 weeks) and monthly injections (for 11 months) of PMO-GF was examined, quantified, and compared with untreated age-matched *mdx* controls as detailed elsewhere.[27] In brief, 1,000 muscle fibers were randomly selected and quantified in a double-blinded manner, with one or more nuclei located centrally defined as centrally nucleated fibers.

Protein Extraction and Western Blot

Protein extraction and western blot were carried out as previously described.[11] Various amounts of protein from *C57BL6* mice as a positive control and 50 μg of total protein from muscles of treated or untreated *mdx* mice were used unless otherwise specified. The quantification is based on band intensity and area with ImageJ software and compared with that from TA muscles of *C57BL6* mice. In brief, the densitometric intensity of each band, including dystrophin and α-actinin, was measured; then the dystrophin values were divided by their respective α-actinin values. The dystrophin/α-actinin ratios of treated samples were normalized to the average *C57BL6* dystrophin/α-actinin ratios (from serial dilutions). Each experiment was performed at least three times (at least three animals).

Functional Grip Strength

Treated and control mice were tested using a commercial grip strength monitor (Chatillon, UK). The procedure was performed as previously described.[11] In brief, each mouse was held 2 cm from the base of the tail, allowed to grip a protruding metal triangle bar attached to the apparatus with their forepaws, and pulled gently until they released their grip. The force exerted was recorded and five sequential tests were carried out for each mouse, averaged at 30 s apart. Subsequently, the readings for force recovery were normalized by the body weight.

Clinical Biochemistry

Serum and plasma were taken from the jugular vein immediately after sacrifice with CO_2 inhalation. Analysis of serum CK, ALP, AST, ALT, serum Cr, urea, and glucose levels was performed by the clinical pathology laboratory (Tianjin Medical University, Metabolic Hospital, Tianjin, China).

Tissue Distribution

Lissamine-labeled PMO was diluted in 100 μL of GF and administered into adult *mdx* mice intravenously at 25 mg/kg for a single injection. Mice treated with labeled PMO were terminally anesthetized 48 hr after injection. Perfusion was performed with 50 mL of cold PBS to wash out free oligonucleotides in circulation. Body-wide muscles, liver, kidney, and brain were harvested for imaging and quantification with IVIS imaging system (PE, USA).

ATP Assay

The extraction of ATP from muscles was adopted and further modified from earlier protocol.[24] In brief, muscles were harvested and snap frozen in liquid nitrogen, and approximately 10–20 mg of 4- to 6-μm-thick cryosections was collected into a 1.5-mL Eppendorf tube. Pre-cooled 0.4 mol/L $HClO_4$ (600 μL) was added to dissolve the sections followed by vortexing for 1 min on ice. The tube was spun for 5 min at 2,000 rpm at 4°C, and the supernatant was transferred to a new tube and another 400 μL of pre-cooled 0.4 mol/L $HClO_4$ was added into the precipitate followed by centrifugation as the previous step.

Subsequently, the supernatant was spun at 4°C for 5 min at 2,000 rpm to remove debris and stored for assay. CellTiter-Glo Luminescent Cell Viability Assay kit (Promega, Fitchburg, WI, USA) was used for measuring levels of ATP in muscles.

OCR Assay

OCR assay was performed with Seahorse extracellular flux analyzer as per the manufacturer's instructions (XF24; Seahorse Bioscience, USA). In brief, primary myoblast cells were isolated from skeletal muscle of *mdx* mice with collagenase II digestion. Cells were seeded at 50,000 cells/well in the Seahorse XF cell culture microplate and incubated in a CO_2 incubator at 37°C for 24 hr. Cells were washed with sodium carbonate-free DMEM (pH 7.4) prior to measurement. Basal and maximal OCRs were measured with the Seahorse extracellular flux analyzer. To measure the maximal OCR, the uncoupler FCCP (5μM) was injected into the cells after the basal respiration measurement. Each experiment was repeated three times with four biological replicates each time.

Masson's Trichrome Staining

Masson's trichrome staining kit (Solarbio, China) was applied for the collagen staining. In brief, series of 8-μm-sections were fixed overnight in Bouin's solution followed by staining with the kit as per the manufacturer's instructions.

Transmission Electron Microscopy

Transmission electron microscopy was performed as described elsewhere.[30] In brief, TA skeletal muscle tissue from age-matched *C57BL6*, *mdx* control, or PMO-GF-treated *mdx* mice were fixed in half-strength Karnovsky's fixative (2.0% paraformaldehyde, 2.5% glutaraldehyde, 0.1 M cacodylate buffer, 3 mM $CaCl_2$ [pH 7.3]), post-fixed for 1 hr in 1.0% OsO4, and then stained with 2% uranyl acetate. Samples were then rinsed and dehydrated through a graded series of alcohol and propylene oxide. Samples were embedded with Eponate resin, and 50-nm sections were cut and mounted on 150 mesh rhodium/copper grids and stained with uranyl acetate and lead citrate. Samples were analyzed, and images were acquired with transmission electron microscopy (Hitachi HT7700; Tokyo, Japan). SSM densities (the number of mitochondria per micron length of sarcolemma) were determined between 20 and 36 electron micrographs of randomly selected fields per mouse with ImageJ. A subsarcolemmal mitochondrion was defined as one that did not have a myofibril between it and the sarcolemma.

ELISA for PMO

ELISA to detect the amount of PMO in muscle tissues was performed as described elsewhere.[48] In brief, DNA probe was designed with sequences complementary to PMO (synthesized by The Beijing Genomics Institute, Beijing, China) as follows: 3′-**CCGGTTT**GGAGCC GAAT**GGACTTTA**-5′, with phosphorothioate ends in bold. The 5′ and 3′ ends of the probes were labeled with digoxigenin and biotin, respectively. Standard PMO samples and muscle tissues (100 mg/mL) were digested with 20 mg/mL proteinase K at 55°C overnight. Following PMO-probe hybridization, the avidin-biotin interaction of the hybridized probe was performed on Pierce NeutrAvidin Coated 96-well plates, Black (Thermo Fisher Scientific, MA, USA). Unhybridized probes were digested with micrococcal nuclease at 10 U/μL (Thermo Fisher Scientific, MA, USA). Then the hybridized probes were reacted with rabbit monoclonal antibody to digoxigenin (Cell Signaling Technology, MA, USA), followed by detection with peroxidase-conjugated goat anti-rabbit IgG (Abcam, Cambridge, UK). Signals from the PMO-hybridized probe were detected at 450 nm with TME Substrate (Solarbio, Beijing, China) in a monochromator EnSpire Multimode plate reader (PerkinElmer, Boston, MA, USA).

Targeted Metabolomics with LC-MS/MS

Targeted metabolomics for energy metabolites were performed by Shanghai Applied Protein Technology (Shanghai, China) with LC-MS/MS as described elsewhere.[49] In brief, 100-mg quadriceps cryosections were placed in EP tubes, and 200 μL of Ultra-pure water and 800 μL of methanol/acetonitrile (1:1, v/v) were added. The sample was grinded by ultrasonic homogenizers, incubated at −20°C for 60 min, and then centrifuged at 14,000 × *g* for 15 min at 4°C. The supernatants were collected and dried with nitrogen; then the lyophilized powder was stored at 80°C prior to analysis. Lyophilized samples were reconstituted by dissolving in 100 μL of solvent mixture containing water/acetonitrile (5:5, v/v). The samples were vortexed for 1 min and centrifuged at 14,000 × *g* for 15 min at 4°C. The supernatants were collected for LC-MS/MS analysis.

Data Analysis

All data are reported as mean values ± SEM. Statistical differences between different treated groups were evaluated by SigmaStat (Systat Software, Chicago, IL, USA). Both parametric and non-parametric analyses were applied, in which the Mann-Whitney rank sum test (Mann-Whitney U test) was used for samples on a non-normal distribution, whereas a two-tailed t test was performed for samples with a normal distribution, respectively.

SUPPLEMENTAL INFORMATION

Supplemental Information includes three figures and can be found with this article online at https://doi.org/10.1016/j.omtn.2018.06.005.

AUTHOR CONTRIBUTIONS

H.Y. conceived the project; G.H. and H.Y. designed the experiments and analyzed the data; H.Y. wrote the manuscript with input from all authors; G.H., C.L., H.N., and X.G. carried out the experiments.

CONFLICTS OF INTEREST

The authors declare no competing financial interests.

ACKNOWLEDGMENTS

The authors acknowledge Dr. Yiqi Seow (Biomedical Sciences Institutes, A*STAR, Singapore) for critical review of the manuscript, and Dr. Wenyan Niu (Tianjin Metabolic Disease Hospital, Tianjin Medical University, Tianjin, China) and Ting Sun (Tianjin Medical University, Tianjin, China) for assistance with the clinical biochemistry assays and tissue imaging. This study was funded by the National

Key R&D Program of China (grant no. 2017YFC1001902), the National Natural Science Foundation of China (grant no. 81672124 and 81671528), the Postdoctoral Science Foundation of China (grant no. 2017M611176), The Science &Technology Development Fund of Tianjin Education Commission for Higher Education (grant no. 2016YD10), and Tianjin Municipal 13th five-year plan (Tianjin Medical University Talent Project).

REFERENCES

1. Aartsma-Rus, A., and Krieg, A.M. (2017). FDA approves eteplirsen for Duchenne muscular dystrophy: the next chapter in the eteplirsen saga. Nucleic Acid Ther. *27*, 1–3.
2. Mendell, J.R., Rodino-Klapac, L.R., Sahenk, Z., Roush, K., Bird, L., Lowes, L.P., Alfano, L., Gomez, A.M., Lewis, S., Kota, J., et al.; Eteplirsen Study Group (2013). Eteplirsen for the treatment of Duchenne muscular dystrophy. Ann. Neurol. *74*, 637–647.
3. Falzarano, M.S., Passarelli, C., Bassi, E., Fabris, M., Perrone, D., Sabatelli, P., Maraldi, N.M., Donà, S., Selvatici, R., Bonaldo, P., et al. (2013). Biodistribution and molecular studies on orally administered nanoparticle-AON complexes encapsulated with alginate aiming at inducing dystrophin rescue in mdx mice. BioMed Res. Int. *2013*, 527418.
4. Rimessi, P., Sabatelli, P., Fabris, M., Braghetta, P., Bassi, E., Spitali, P., Vattemi, G., Tomelleri, G., Mari, L., Perrone, D., et al. (2009). Cationic PMMA nanoparticles bind and deliver antisense oligoribonucleotides allowing restoration of dystrophin expression in the mdx mouse. Mol. Ther. *17*, 820–827.
5. Sirsi, S.R., Schray, R.C., Wheatley, M.A., and Lutz, G.J. (2009). Formulation of polylactide-co-glycolic acid nanospheres for encapsulation and sustained release of poly(ethylene imine)-poly(ethylene glycol) copolymers complexed to oligonucleotides. J. Nanobiotechnology *7*, 1.
6. Williams, J.H., Schray, R.C., Sirsi, S.R., and Lutz, G.J. (2008). Nanopolymers improve delivery of exon skipping oligonucleotides and concomitant dystrophin expression in skeletal muscle of mdx mice. BMC Biotechnol. *8*, 35.
7. Wu, B., Moulton, H.M., Iversen, P.L., Jiang, J., Li, J., Li, J., Spurney, C.F., Sali, A., Guerron, A.D., Nagaraju, K., et al. (2008). Effective rescue of dystrophin improves cardiac function in dystrophin-deficient mice by a modified morpholino oligomer. Proc. Natl. Acad. Sci. USA *105*, 14814–14819.
8. Jearawiriyapaisarn, N., Moulton, H.M., Buckley, B., Roberts, J., Sazani, P., Fucharoen, S., Iversen, P.L., and Kole, R. (2008). Sustained dystrophin expression induced by peptide-conjugated morpholino oligomers in the muscles of mdx mice. Mol. Ther. *16*, 1624–1629.
9. Yin, H., Moulton, H.M., Seow, Y., Boyd, C., Boutilier, J., Iverson, P., and Wood, M.J. (2008). Cell-penetrating peptide-conjugated antisense oligonucleotides restore systemic muscle and cardiac dystrophin expression and function. Hum. Mol. Genet. *17*, 3909–3918.
10. Yin, H., Saleh, A.F., Betts, C., Camelliti, P., Seow, Y., Ashraf, S., Arzumanov, A., Hammond, S., Merritt, T., Gait, M.J., and Wood, M.J. (2011). Pip5 transduction peptides direct high efficiency oligonucleotide-mediated dystrophin exon skipping in heart and phenotypic correction in mdx mice. Mol. Ther. *19*, 1295–1303.
11. Han, G., Gu, B., Cao, L., Gao, X., Wang, Q., Seow, Y., Zhang, N., Wood, M.J., and Yin, H. (2016). Hexose enhances oligonucleotide delivery and exon skipping in dystrophin-deficient mdx mice. Nat. Commun. *7*, 10981.
12. Cao, L., Han, G., Lin, C., Gu, B., Gao, X., Moulton, H.M., Seow, Y., and Yin, H. (2016). Fructose promotes uptake and activity of oligonucleotides with different chemistries in a context-dependent manner in mdx mice. Mol. Ther. Nucleic Acids *5*, e329.
13. Alter, J., Lou, F., Rabinowitz, A., Yin, H., Rosenfeld, J., Wilton, S.D., Partridge, T.A., and Lu, Q.L. (2006). Systemic delivery of morpholino oligonucleotide restores dystrophin expression bodywide and improves dystrophic pathology. Nat. Med. *12*, 175–177.
14. Goyenvalle, A., Griffith, G., Babbs, A., El Andaloussi, S., Ezzat, K., Avril, A., Dugovic, B., Chaussenot, R., Ferry, A., Voit, T., et al. (2015). Functional correction in mouse models of muscular dystrophy using exon-skipping tricyclo-DNA oligomers. Nat. Med. *21*, 270–275.
15. Wu, B., Xiao, B., Cloer, C., Shaban, M., Sali, A., Lu, P., Li, J., Nagaraju, K., Xiao, X., and Lu, Q.L. (2011). One-year treatment of morpholino antisense oligomer improves skeletal and cardiac muscle functions in dystrophic mdx mice. Mol. Ther. *19*, 576–583.
16. Yin, H., Betts, C., Saleh, A.F., Ivanova, G.D., Lee, H., Seow, Y., Kim, D., Gait, M.J., and Wood, M.J. (2010). Optimization of peptide nucleic acid antisense oligonucleotides for local and systemic dystrophin splice correction in the mdx mouse. Mol. Ther. *18*, 819–827.
17. Deconinck, N., and Dan, B. (2007). Pathophysiology of duchenne muscular dystrophy: current hypotheses. Pediatr. Neurol. *36*, 1–7.
18. Hoffman, E.P., Bronson, A., Levin, A.A., Takeda, S., Yokota, T., Baudy, A.R., and Connor, E.M. (2011). Restoring dystrophin expression in duchenne muscular dystrophy muscle progress in exon skipping and stop codon read through. Am. J. Pathol. *179*, 12–22.
19. Lu, Q.L., Rabinowitz, A., Chen, Y.C., Yokota, T., Yin, H., Alter, J., Jadoon, A., Bou-Gharios, G., and Partridge, T. (2005). Systemic delivery of antisense oligoribonucleotide restores dystrophin expression in body-wide skeletal muscles. Proc. Natl. Acad. Sci. USA *102*, 198–203.
20. Malerba, A., Sharp, P.S., Graham, I.R., Arechavala-Gomeza, V., Foster, K., Muntoni, F., Wells, D.J., and Dickson, G. (2011). Chronic systemic therapy with low-dose morpholino oligomers ameliorates the pathology and normalizes locomotor behavior in mdx mice. Mol. Ther. *19*, 345–354.
21. Timpani, C.A., Hayes, A., and Rybalka, E. (2015). Revisiting the dystrophin-ATP connection: how half a century of research still implicates mitochondrial dysfunction in Duchenne Muscular Dystrophy aetiology. Med. Hypotheses *85*, 1021–1033.
22. Even, P.C., Decrouy, A., and Chinet, A. (1994). Defective regulation of energy metabolism in mdx-mouse skeletal muscles. Biochem. J. *304*, 649–654.
23. Pant, M., Sopariwala, D.H., Bal, N.C., Lowe, J., Delfín, D.A., Rafael-Fortney, J., and Periasamy, M. (2015). Metabolic dysfunction and altered mitochondrial dynamics in the utrophin-dystrophin deficient mouse model of duchenne muscular dystrophy. PLoS ONE *10*, e0123875.
24. Ronzoni, E., Wald, S., Berg, L., and Ramsey, R. (1958). Distribution of high energy phosphate in normal and dystrophic muscle. Neurology *8*, 359–368.
25. Ehmsen, J., Poon, E., and Davies, K. (2002). The dystrophin-associated protein complex. J. Cell Sci. *115*, 2801–2803.
26. Ozawa, E., Hagiwara, Y., and Yoshida, M. (1999). Creatine kinase, cell membrane and Duchenne muscular dystrophy. Mol. Cell. Biochem. *190*, 143–151.
27. Narita, S., and Yorifuji, H. (1999). Centrally nucleated fibers (CNFs) compensate the fragility of myofibers in mdx mouse. Neuroreport *10*, 3233–3235.
28. Brazeau, G.A., Mathew, M., and Entrikin, R.K. (1992). Serum and organ indices of the mdx dystrophic mouse. Res. Commun. Chem. Pathol. Pharmacol. *77*, 179–189.
29. Marrocco, V., Fiore, P., Benedetti, A., Pisu, S., Rizzuto, E., Musarò, A., Madaro, L., Lozanoska-Ochser, B., and Bouché, M. (2017). Pharmacological inhibition of PKCθ counteracts muscle disease in a mouse model of Duchenne muscular dystrophy. EBioMedicine *16*, 150–161.
30. Percival, J.M., Siegel, M.P., Knowels, G., and Marcinek, D.J. (2013). Defects in mitochondrial localization and ATP synthesis in the mdx mouse model of Duchenne muscular dystrophy are not alleviated by PDE5 inhibition. Hum. Mol. Genet. *22*, 153–167.
31. Mastaglia, F.L., Papadimitriou, J.M., and Kakulas, B.A. (1970). Regeneration of muscle in Duchenne muscular dystrophy: an electron microscope study. J. Neurol. Sci. *11*, 425–444.
32. Rybalka, E., Timpani, C.A., Cooke, M.B., Williams, A.D., and Hayes, A. (2014). Defects in mitochondrial ATP synthesis in dystrophin-deficient mdx skeletal muscles may be caused by complex I insufficiency. PLoS ONE *9*, e115763.
33. Hood, D.A. (2001). Invited review: contractile activity-induced mitochondrial biogenesis in skeletal muscle. J. Appl. Physiol. *90*, 1137–1157.
34. Godin, R., Daussin, F., Matecki, S., Li, T., Petrof, B.J., and Burelle, Y. (2012). Peroxisome proliferator-activated receptor γ coactivator1- gene α transfer restores mitochondrial biomass and improves mitochondrial calcium handling in post-necrotic mdx mouse skeletal muscle. J. Physiol. *590*, 5487–5502.

35. Jahnke, V.E., Van Der Meulen, J.H., Johnston, H.K., Ghimbovschi, S., Partridge, T., Hoffman, E.P., and Nagaraju, K. (2012). Metabolic remodeling agents show beneficial effects in the dystrophin-deficient mdx mouse model. Skelet. Muscle *2*, 16.

36. Ferlini, A., Sabatelli, P., Fabris, M., Bassi, E., Falzarano, S., Vattemi, G., Perrone, D., Gualandi, F., Maraldi, N.M., Merlini, L., et al. (2010). Dystrophin restoration in skeletal, heart and skin arrector pili smooth muscle of mdx mice by ZM2 NP-AON complexes. Gene Ther. *17*, 432–438.

37. Cutró, A.C., Montich, G.G., and Roveri, O.A. (2014). Effect of carbonylcyanide-4-(trifluoromethoxy)phenylhydrazone (FCCP) on the interaction of 1-anilino-8-naphthalene sulfonate (ANS) with phosphatidylcholine liposomes. J. Bioenerg. Biomembr. *46*, 119–125.

38. Hartman, M.L., Shirihai, O.S., Holbrook, M., Xu, G., Kocherla, M., Shah, A., Fetterman, J.L., Kluge, M.A., Frame, A.A., Hamburg, N.M., and Vita, J.A. (2014). Relation of mitochondrial oxygen consumption in peripheral blood mononuclear cells to vascular function in type 2 diabetes mellitus. Vasc. Med. *19*, 67–74.

39. Stein, L.R., and Imai, S. (2012). The dynamic regulation of NAD metabolism in mitochondria. Trends Endocrinol. Metab. *23*, 420–428.

40. Martens, M.E., Jankulovska, L., Neymark, M.A., and Lee, C.P. (1980). Impaired substrate utilization in mitochondria from strain 129 dystrophic mice. Biochim. Biophys. Acta *589*, 190–200.

41. Chen, Y.W., Zhao, P., Borup, R., and Hoffman, E.P. (2000). Expression profiling in the muscular dystrophies: identification of novel aspects of molecular pathophysiology. J. Cell Biol. *151*, 1321–1336.

42. Dudley, R.W., Khairallah, M., Mohammed, S., Lands, L., Des Rosiers, C., and Petrof, B.J. (2006). Dynamic responses of the glutathione system to acute oxidative stress in dystrophic mouse (mdx) muscles. Am. J. Physiol. Regul. Integr. Comp. Physiol. *291*, R704–R710.

43. Zatz, M., Rapaport, D., Vainzof, M., Passos-Bueno, M.R., Bortolini, E.R., Pavanello, Rde.C., and Peres, C.A. (1991). Serum creatine-kinase (CK) and pyruvate-kinase (PK) activities in Duchenne (DMD) as compared with Becker (BMD) muscular dystrophy. J. Neurol. Sci. *102*, 190–196.

44. Chi, M.M., Hintz, C.S., McKee, D., Felder, S., Grant, N., Kaiser, K.K., and Lowry, O.H. (1987). Effect of Duchenne muscular dystrophy on enzymes of energy metabolism in individual muscle fibers. Metabolism *36*, 761–767.

45. Boucek, R.J., Jr., Kasselberg, A.G., Boerth, R.C., Parrish, M.D., and Graham, T.P., Jr. (1982). Myocardial injury in infants with congenital heart disease: evaluation by creatine kinase MB isoenzyme analysis. Am. J. Cardiol. *50*, 129–135.

46. Gebski, B.L., Mann, C.J., Fletcher, S., and Wilton, S.D. (2003). Morpholino antisense oligonucleotide induced dystrophin exon 23 skipping in mdx mouse muscle. Hum. Mol. Genet. *12*, 1801–1811.

47. Mann, C.J., Honeyman, K., Cheng, A.J., Ly, T., Lloyd, F., Fletcher, S., Morgan, J.E., Partridge, T.A., and Wilton, S.D. (2001). Antisense-induced exon skipping and synthesis of dystrophin in the mdx mouse. Proc. Natl. Acad. Sci. USA *98*, 42–47.

48. Burki, U., Keane, J., Blain, A., O'Donovan, L., Gait, M.J., Laval, S.H., and Straub, V. (2015). Development and application of an ultrasensitive hybridization-based ELISA method for the determination of peptide-conjugated phosphorodiamidate morpholino oligonucleotides. Nucleic Acid Ther. *25*, 275–284.

49. Filigenzi, M.S., Tor, E.R., Poppenga, R.H., Aston, L.A., and Puschner, B. (2007). The determination of melamine in muscle tissue by liquid chromatography/tandem mass spectrometry. Rapid Commun. Mass Spectrom. *21*, 4027–4032.